



ELSEVIER

Available online at www.sciencedirect.com

SCIENCE @ DIRECT®

Proceedings of the Combustion Institute 30 (2005) 1565–1573

Proceedings
of the
Combustion
Institute

www.elsevier.com/locate/proci

A technique for extrapolating absorption coefficient measurements to high temperatures

K. Wakatsuki^{a,*}, S.P. Fuss^b, A. Hamins^c, M.R. Nyden^c

^a Department of Mechanical Engineering, University of Maryland, College Park, MD 20742, USA

^b Fire Research Laboratory, Bureau of Alcohol, Tobacco, Firearms and Explosives, Beltsville, MD 20705, USA

^c Building and Fire Research Laboratory, National Institute of Standards and Technology, Gaithersburg, MD 20899, USA

Abstract

An extrapolation technique that provides semi-quantitative estimates for the infrared absorption coefficients of gaseous fuels at temperatures beyond those for which measurements are generally practical (>700 K) is presented. The new method is based on a simplified expression for molecular line intensities consisting of three fitting parameters and two variables (temperature and frequency). The accuracy of the extrapolations was tested first by comparing predictions of absorption coefficients for CO, CO₂, and H₂O vapor to the corresponding values obtained directly from the HITEMP molecular database. Finally, to establish the practical utility of the method, the spectrum of propane at 1000 K obtained from the extrapolation technique was compared to actual experimental measurements.

© 2004 The Combustion Institute. Published by Elsevier Inc. All rights reserved.

Keywords: Radiation; Infrared spectroscopy; High temperature; Absorption coefficients; Extrapolation

1. Introduction

The transfer of thermal energy between the flames and fuel in a combusting system is mediated by the absorption and emission of infrared radiation (IR). Consequently, the spectroscopic properties of the fuel and gas phase combustion intermediates must be known (in the form of calibration spectra for the gases of interest at fire temperatures) to accurately model the transfer of radiation in fires and incinerators. In principle, this information can be obtained from non-intrusive measurements of the attenuation in the intensity of IR radiation from an external source, such

as from a Fourier transform infrared (FTIR) spectrometer. Unfortunately, it is difficult to measure calibration quality spectra at temperatures above 700 K due to oxidation and thermal degradation of the infrared windows. Furthermore, since the IR spectra of gas phase molecules undergo dramatic changes with increasing temperature, the common strategy of using spectra measured at room temperature to approximate high temperature absorption coefficients [1] yields unacceptable errors.

Much attention has been focused on how soot affects radiation in hydrocarbon fires. Although the effects of soot are presumed to be more significant, it is nevertheless true that relatively little is known about the absorption properties of large hydrocarbon molecules near the fuel source. In work directed at measuring the radiative feedback to the fuel surface in

* Corresponding author. Fax: +1 301 975 4052.

E-mail address: kaoru.wakatsuki@nist.gov (K. Wakatsuki).

PMMA pool fires, DeRis [2] concluded that “it is critically important for fire researchers to develop accurate and convenient ways to measure absorption–emission coefficients for fuels.” This has motivated several recent studies on fuel absorption at elevated temperatures [3–7]. The focus of this investigation was to develop a semi-quantitative method to extrapolate absorption coefficients, obtained for temperatures up to 700 K, to the higher temperatures (1000 K) that are required to describe the transfer of radiation between the flame zone and fuel-rich core.

2. Extrapolation technique

According to the Beer–Lambert law, the absorption coefficient, κ_v , at any wavenumber, ν , can be expressed in terms of measurable quantities as

$$\kappa_v = \frac{-\ln(\tau_\nu)}{pL}, \quad (1)$$

where τ_ν is the spectral transmittance, p is the partial pressure of the absorbing specie (Pa), and L is the measurement path length (m). From a fundamental perspective [8], the absorption coefficient is the product of line intensity (S), line shape ($g(\nu - \nu_0)$), and the number of absorbing molecules per unit volume and pressure:

$$\kappa_v = Sg(\nu - \nu_0)N_L \left(\frac{296}{T}\right), \quad (2)$$

where ν_0 is the center of an absorbing line in wavenumber and N_L is Loschmidts' number ($N_L = 2.447 \cdot 10^{19}$ molecules/cm³/kPa at 296 K). For applications at atmospheric pressure and moderate temperatures, the Lorentzian line shape is generally applied:

$$g(\nu - \nu_0) = \frac{(\gamma_p/\pi)}{(\nu - \nu_0)^2 + \gamma_p^2}, \quad (3)$$

where γ_p is the pressure-broadened line half width:

$$\gamma_p = g \left(\frac{296}{T}\right)^n P_t, \quad (4)$$

where P_t is the total pressure and g is a broadening parameter (cm⁻¹/kPa), and n is the air-broadened linewidth parameter.

The line intensity (S) corresponds to the product of the quantum mechanical probability for the transition and the population difference between the initial (absorption) and final (emission) states [10]:

$$S = \left\{ \frac{8\pi^3}{3hc} \right\} \nu \left\{ \frac{|\bar{R}|^2}{g_1} \right\} g_i I_a \left[1 - \exp\left(-\frac{h\nu}{kT}\right) \right] \times g_1 \exp\left(-\frac{E'}{kT}\right) / Q 10^{36}. \quad (5)$$

Here, h and k are the Planck and Boltzmann constants, respectively, c is the speed of light, E' is the energy of the lower state, \bar{R} is the transition moment, and $h\nu$ is the difference in energy between the upper and lower states. The second bracketed term is the quantum mechanical transition probability, where g_1 is the degeneracy of the lower state. Finally, I_a is the isotope fraction, g_i is the nuclear spin degeneracy, and Q is the rotational partition sum. Combining Eqs. (2)–(5) yields:

$$k_v = \left\{ \frac{8 \cdot \pi^3}{3hc} \right\} \nu \left\{ \frac{|\bar{R}|^2}{g_1} \right\} g_i I_a \times \left[1 - \exp\left(-\frac{h\nu}{kT}\right) \right] g_1 \exp\left(-\frac{E'}{kT}\right) \frac{g}{\pi} \left(\frac{296}{T}\right)^n \times P_t \cdot N_L \cdot \left(\frac{296}{T}\right) / Q 10^{36} \times \left[(\nu - \nu_0)^2 + \left(g \left(\frac{296}{T}\right)^n P_t \right)^2 \right], \quad (6)$$

where P_t is the total pressure and g is a broadening parameter (cm⁻¹/kPa).

The approach taken in this study was to simplify this expression to a form suitable for fitting the absorption coefficients measured over a range of temperatures. This was achieved by reducing Eq. (6) to an expression containing three fit parameters (S_0 , E' , and p) and two variables (ν and T). The values of the absorption coefficients at higher temperatures, which are difficult to measure, can then be estimated by extrapolation.

The terms with negligible temperature or frequency dependence were consolidated into S_0 as indicated in Eq. (7)

$$S_0 = \frac{\left\{ \frac{8\pi^2}{3hc} \right\} \left\{ \frac{|\bar{R}|^2}{g_1} \right\} g_i I_a g_1 N_L}{296^{n-1} 10^{36} g P_t \left(\frac{Q}{T^{m/2}}\right)}. \quad (7)$$

As a first approximation, we also ignored the explicit contributions from overlapping rotational lines (i.e., we set $\nu = \nu_0$) so that the effects of the Lorentzian line shape functions are effectively subsumed into the S_0 and T^p (see Eq. (8)) terms. Since the temperature dependence of each rotational transition is unique, this approximation is likely to result in larger errors when the resolution of the measurements is not sufficient to differentiate between the individual lines. After substituting $E' = h\nu_r = 1.439 \nu_r$ for the energy of the lower state, Eq. (6) becomes:

$$k_v = \frac{S_0 \nu \left[1 - \exp\left(-\frac{1.439\nu}{T}\right) \right] \exp\left(-\frac{1.439\nu_r}{T}\right)}{T^p}. \quad (8)$$

In this expression temperature, T (K), and wavenumber, ν (cm⁻¹), are independent variables and the parameters S_0 , ν_r , and p were fit over a range of temperatures at each wavenumber.

3. Extrapolation data processing

3.1. HITEMP database (CO , CO_2 , and H_2O)

Absorption data for CO , CO_2 , and H_2O were obtained from the HITEMP database [10]. HITEMP is the high temperature analog of the HITRAN database, which is an extensive compilation of molecular line absorption data for 38 species [9]. The accuracy of the spectra derived from the HITEMP database for applications to combusting systems at temperatures exceeding 1000 K has already been examined by others [11].

3.2. Experiment

A Mattson Galaxy 7020 FTIR spectrometer¹ was modified so that the IR beam from a global source passes through the interferometer but is then diverted outside the spectrometer, bypassing the standard sample compartment and detector. The absorption spectra were measured at 1 cm^{-1} resolution and signal averaged over 128 scans. The IR beam travels along the axis of a quartz flow cell, which is located inside a tube furnace, and onto an external mercury cadmium telluride (MCT) detector (MI0465, Graseby Infrared). A diagram of our experimental setup is shown in Fig. 1. The entire optical path, including the spectrometer and external detector chamber, was purged with N_2 to eliminate absorption from ambient water vapor and CO_2 . The interferometer is equipped with corner-cube optics. This arrangement minimizes the effect of sample emission on the transmission measurements [12]. This was confirmed by measuring the emissions (with the source blocked) from the heated (1000 K) cell containing propane gas, which were found to be negligible. The furnace (Lindberg/Blue M HTF 53347C) has three heating zones designed to maintain a uniform temperature over the full length ($31.75 \pm 0.01\text{ cm}$) of the cell (inner diameter = 2.54 cm). The gas temperatures were measured with K-type thermocouples at the inlet and outlet of the cell. The temperature difference between two thermocouples was typically about 5 K, which was considered acceptable for the purposes of this investigation. The temperature of the windows was kept below 700 K to prevent oxidation of the ZnSe directing a jet of N_2 on the outside of the windows as seen in Fig. 1. The ends of

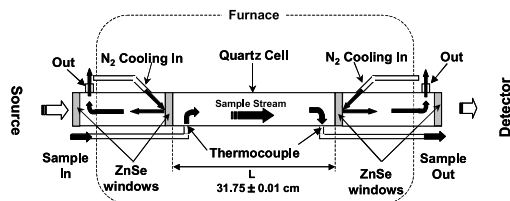


Fig. 1. Diagram of experiment setup.

the quartz cell were sealed by a graphite sheet (0.1 cm thickness) between zinc selenide (ZnSe) laser grade windows (0.3 cm thickness) and the cell. An absolute pressure transducer was installed just before the gas cell to monitor the gas pressure during the measurements, which was maintained at 101.3 kPa. Mixtures containing $0.101 \pm 0.002\text{ kPa}$, $0.253 \pm 0.005\text{ kPa}$, and $0.405 \pm 0.008\text{ kPa}$ of propane (CP Grade, Matheson) in N_2 (99.95% Super Dry) were made by regulating the flow of these gases into the cell using mass flow controllers.

Comparisons of our extrapolation technique to experimental measurements were performed for propane at 800 and 1000 K based on fits determined from measurements made at temperatures of 300, 400, 450, 500, and 600 K.

4. Accuracy assessment

In assessing the accuracy of our extrapolations, integrated absorption coefficients from the extrapolated spectra are compared to the corresponding values from the experimental (or HITEMP) spectra. The integrated absorption coefficient was calculated according to Eq. (9):

$$\int_{\nu_1}^{\nu_2} \kappa_{\nu} d\nu = \frac{-\int_{\nu_1}^{\nu_2} \ln(\tau_{\nu}) d\nu}{\rho L} \quad (9)$$

In this equation, ν_1 and ν_2 are the frequencies corresponding to the band limits. These limits are given in Tables 1 and 2 for the HITEMP and measured data, respectively. Integrated absorption coefficients for the HITEMP species were based on the following concentrations: CO (0.101 kPa), H_2O (1.01 kPa), and CO_2 (0.341 kPa). In the case of propane, an average integrated absorption coefficient was obtained from spectra of the three concentrations (0.101, 0.253, and 0.405 kPa). The accuracies of the extrapolations are assessed according to Eq. (10). The relative errors are determined by taking the ratio of the difference between the integrated absorption coefficients obtained from the extrapolations and the “actual” values obtained (either from HITEMP for CO , H_2O , and CO_2 or experimental spectra for C_3H_8) and dividing by the “actual” values.

¹ Certain commercial equipment, materials, or software are identified in this manuscript to specify adequately the nature of the research. Such identification does not imply recommendation or endorsement by the National Institute of Standards and Technology, nor does it imply that the materials or equipment are necessarily the best available for the purpose.

Table 1
Summary of errors in the HITEMP extrapolations

Molecule (res. cm ⁻¹)	Integration range (cm ⁻¹)	Temperature (K)			
		300		1000	
		Error in integrated values (%)		RMS of the residual	
CO (1)	2150–2270	-0.1	3.6	1.33 E ⁻³	1.11 E ⁻³
CO (4)	2150–2270	0.3	-0.3	2.04 E ⁻⁴	1.10 E ⁻³
H ₂ O (4)	3500–4000	-0.02	3.6	2.09 E ⁻³	4.85 E ⁻³
CO ₂ (0.5)	2250–2350	-2.1	-0.7	3.06 E ⁻²	1.45 E ⁻²
CO ₂ (4)	2250–2350	-1.1	1.3	1.36 E ⁻²	1.18 E ⁻¹

Table 2
Errors in the integrated absorption coefficients for propane at 1 cm⁻¹ resolution

Integration range (cm ⁻¹)	Temperature (K)					
	300			800		
	Integrated absorption coefficient (Pa ⁻¹ m ⁻¹)			Error in integrated values (%)		
	300	800	1000	300	800	1000
	Upper: extrapolation					
	Lower: experiment					
2700–2850	0.030	0.022	0.020	3.5	-41.1	-40.8
Right wing	0.029	0.037	0.033			
2850–3050	1.064	0.324	0.244	-1.9	-15.9	-4.3
Band center	1.084	0.385	0.255			
3050–3200	0.014	0.013	0.011	16.7	-53.7	-59.0
Left wing	0.012	0.027	0.026			

$$\text{Error (\%)} = \frac{\int_{\Delta\nu} \kappa_{\nu(\text{FIT})} d\nu - \int_{\Delta\nu} \kappa_{\nu(\text{HITEMP or Experiment})} d\nu}{\int_{\Delta\nu} \kappa_{\nu(\text{HITEMP or Experiment})} d\nu} \times 100. \quad (10)$$

Chu et al. [13] report that line intensity variations of the order of $\pm 10\%$ can be frequently found in comparisons of quantitative reference spectra obtained from FTIR measurements. This is consistent with the variations we observed in repetitive measurements of the spectrum of propane at elevated temperatures.

5. Extrapolation results

As a first attempt, the accuracy of the extrapolation procedure was examined without introducing complications due to experimental errors. Extrapolations of the CO, CO₂, and H₂O spectra to a temperature of 1000 K (based on parameters determined by fitting Eq. (8) to HITEMP spectra for temperatures 300, 400, 450, 500, and 600 K) were compared to the corresponding spectra at 1000 K generated directly from the HITEMP database. This exercise provides an estimate of the magnitude of the errors resulting from the simplifications introduced in representing Eq. (6) by Eq. (8). The practical utility of using this methodology in conjunction with

experimental measurements is demonstrated by comparing predictions at 800 and 1000 K (based on fits of spectra measured at lower temperatures) with measurements at 800 and 1000 K for absorption by the C–H stretching region in propane.

5.1. Carbon monoxide

Parameters were fit for the R branch of the 4.7 μm CO band, over the range from 2150 to 2270 cm⁻¹. The data were generated at a resolution of 1 cm⁻¹, resulting in an average spacing of 0.482 cm⁻¹. This was sufficiently high that the individual lines in the band were resolved. Fig. 2A is a comparison of the extrapolated absorption coefficient from Eq. (8) to the one from HITEMP at 300 K. The difference in the integrated absorption between the original and fit data, obtained from Eq. (10), is less than -0.1%. The small error is expected because the reference spectrum was included in the training set. In Fig. 2B, however, the extrapolated absorption coefficients are compared to the HITEMP data at 1000 K, which is 400 K above the highest temperature spectrum used in the fitting procedure. The difference in the integrated absorbance at this temperature is still only 3.6%. While this agreement may be a little misleading because there is clearly a cancellation of errors, the magnitudes of the residuals (Fig. 3)

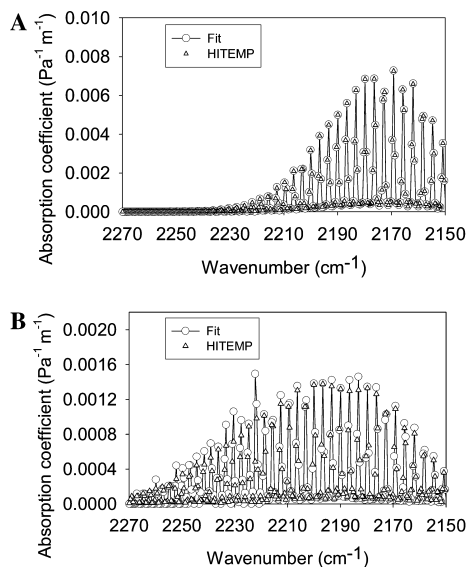


Fig. 2. Comparison of CO spectral absorption coefficient between HITEMP and data calculated using Eq. (8) with fit parameters at 1 cm^{-1} resolution: (A) 300 K, (B) 1000 K.

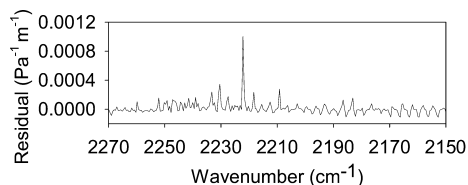


Fig. 3. Residual ($\kappa_{\text{Fit}} - \kappa_{\text{HITEMP}}$) for CO at 1000 K. This represents the difference between the data sets shown in Fig. 2.

are on average at least an order of magnitude smaller than the absorbance values.

The spectra of heavier molecules are not as well resolved at elevated temperatures as is the CO spectrum shown in Fig. 2. Closely spaced broadened lines will, in effect, smear out distinguishable line structure. Since this is the case for many fuels, it is important to investigate the effect of reducing the resolution on the accuracy of the extrapolations. Figures 4A and B compare the extrapolated absorption coefficients and HITEMP data at 300 K and 1000 K measured at 4 cm^{-1} resolution. At this resolution, the CO line structure is gone, and the band appears as a continuous absorption. The fit procedure was carried out using these data with similar results as the higher resolution case. The integrated absorbance at 1000 K using the fit parameters differed from the HITEMP data by only -0.28% . The errors in the temperature extrapolations for CO appear to

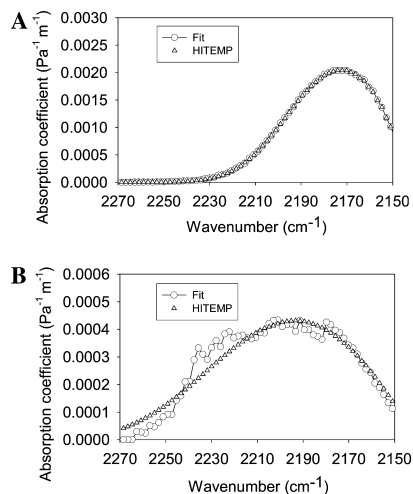


Fig. 4. Comparison of CO spectral absorption coefficient between HITEMP and data calculated using Eq. (8) with fit parameter at 4 cm^{-1} resolution: (A) 300 K, (B) 1000 K.

remain tractable upon de-resolving the spectrum, even though the contributions from overlapping rotational lines were not explicitly accounted for in the derivation of Eq. (8).

5.2. Water vapor

Parameters were fit to lines in the $2.7\text{ }\mu\text{m}$ water band, over the range between 3500 and 4000 cm^{-1} . The temperatures used were the same as those in the CO case. The water absorption data were generated from the HITEMP database at a resolution of 4 cm^{-1} , resulting in an average data spacing of 1.93 cm^{-1} . At this resolution, most of the line structure is still visible in this band. Figure 5A is a comparison of extrapolated absorption coefficient from Eq. (8) to the one from HITEMP at 300 K, using the parameters generated in the fit. The results of this comparison were comparable to those from the CO fit at 300 K. The difference in the integrated absorbance was -0.02% . Again, a small error is anticipated because the parameters were fit to data at this temperature. However, the comparison is still favorable at 1000 K, where the difference in the integrated absorbance is only 3.6% . This result is shown in Fig. 5B. The residuals are shown as a function of wavenumber in Fig. 6.

5.3. Carbon dioxide

The accuracy of the extrapolation method for the $4.3\text{ }\mu\text{m}$ band in CO_2 over the spectral range 2250 – 2350 cm^{-1} (P branch) was also examined. The procedure was carried out using data at two

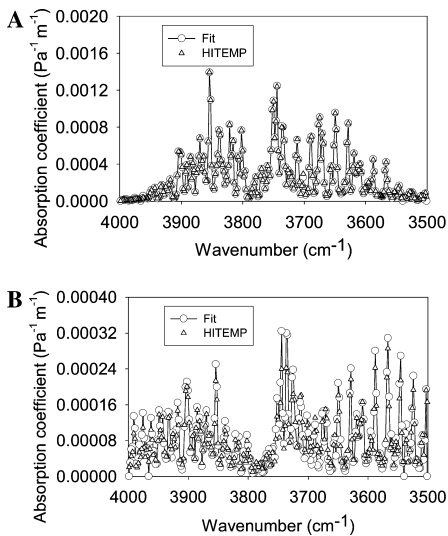


Fig. 5. Comparison of water vapor spectral absorption coefficient between HITEMP and data calculated using Eq. (8) with fit parameters at 1 cm^{-1} resolution: (A) 300 K, (B) 1000 K.

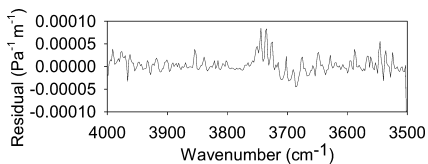


Fig. 6. Residual ($\kappa_{\text{Fit}} - \kappa_{\text{HITEMP}}$) for H_2O at 1000 K. This represents the difference between the data sets shown in Fig. 5.

resolutions: 0.5 and 4 cm^{-1} , resulting in average data spacing of 0.241 cm^{-1} and 1.93 cm^{-1} , respectively.

The HITEMP and fit data at $T = 300\text{ K}$ and 0.5 cm^{-1} resolution are compared in Fig. 7A. In this case, the difference in the integrated absorption coefficient was -2.1% . At 1000 K, the difference at 0.5 cm^{-1} resolution was only -0.7% . While the error in the integrated absorbance is small, a frequency resolved comparison, as indicated by the residual spectrum in Fig. 8, does reveal a small, but noticeable, systematic error between 2270 and 2300 cm^{-1} . At 4 cm^{-1} resolution, the difference in the integrated absorption coefficient is -1.1% and 1.3% at 300 and 1000 K, respectively. The discrepancies are apparent in the comparison shown in Fig. 9.

A summary of the integrated and residual RMS errors for the extrapolations of the HITEMP data is presented in Table 1. Although the cancellation of positive and negative errors

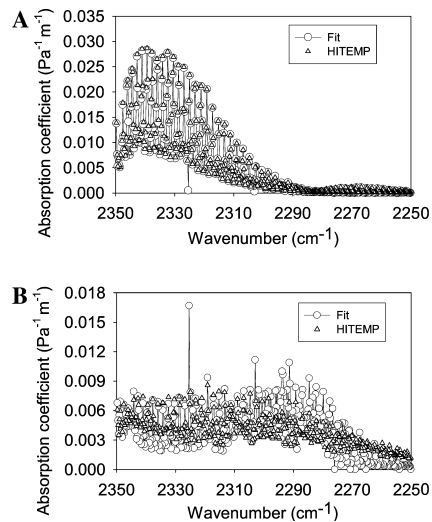


Fig. 7. Comparison of CO_2 spectral absorption coefficient at 300 K between HITEMP and data calculated using Eq. (8) with fit parameters at 0.5 cm^{-1} resolution: (A) 300 K, (B) 1000 K.

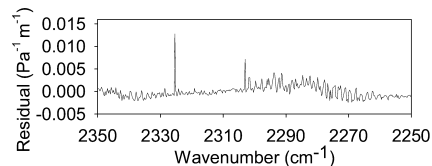


Fig. 8. Residual ($\kappa_{\text{Fit}} - \kappa_{\text{HITEMP}}$) for CO_2 at 1000 K. This represents the difference between the data sets shown in Fig. 7.

makes it difficult to discern a pattern in the discrepancies between the integrated absorption coefficients obtained from direct calculation and the extrapolation, it does appear that the RMS errors grow more rapidly with temperature in the extrapolations from the lower resolution spectra. However, in either case, the errors in the extrapolations are comparable to the experimental uncertainties reported by Chu [13].

5.4. Propane (C_3H_8)

Figure 10 shows how the absorption coefficient for propane varies with temperature. The band broadens with increasing temperature as higher energy rotational states become populated. Furthermore, the peak absorption drops by more than an order of magnitude from 300 to 1000 K. These changes in the shape and intensity of the absorption band are captured in the extrapolations.

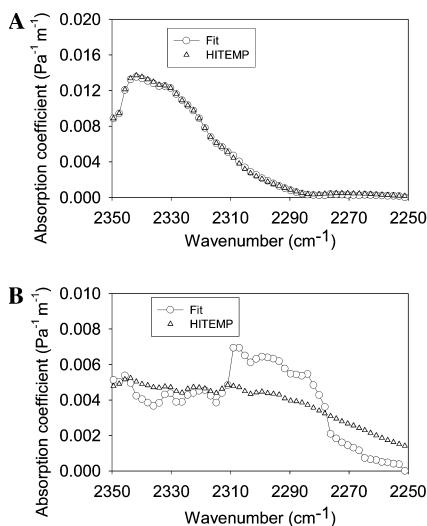


Fig. 9. Comparison of CO₂ spectral absorption coefficient at 1000 K between HITEMP and data calculated using Eq. (8) with fit parameters at 4 cm⁻¹ resolution: (A) 300 K, (B) 1000 K.

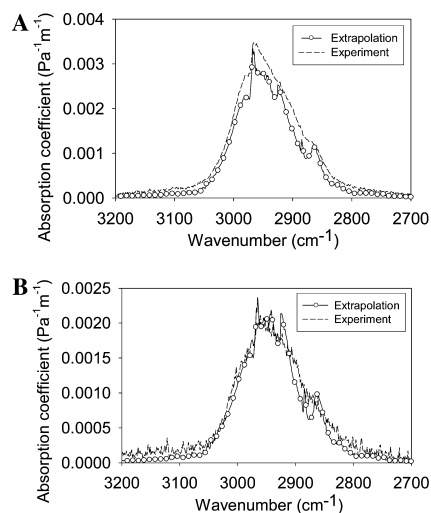


Fig. 11. Comparison of C₃H₈ mean spectral absorption coefficient between Experiment and data calculated using Eq. (8) with fit parameters at 1 cm⁻¹ resolution: (A) 800 K, (B) 1000 K.

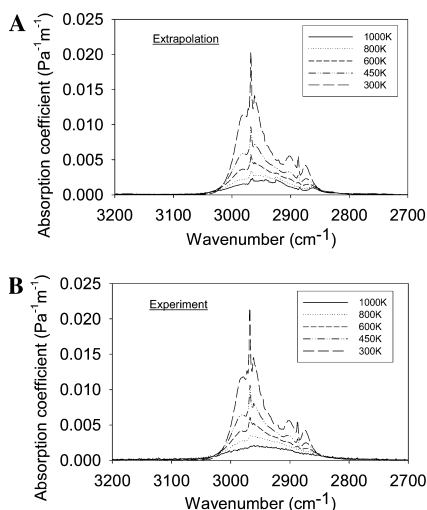


Fig. 10. Comparison of C₃H₈ mean spectral absorption coefficient between Experiment and data calculated using Eq. (8) with fit parameters at 1 cm⁻¹ resolution: (A) extrapolation, (B) experiment.

The extrapolated absorption coefficients at 800 K (A) and 1000 K (B) are compared to the corresponding experimental values in Fig. 11. Although there is at least qualitative agreement, a more detailed comparison reveals that the extrapolations exhibit more structure and underestimate the absorbance at the wings of the bands. The residuals at 1000 K are shown as a function of wavenumber in Fig. 12. The fine structure

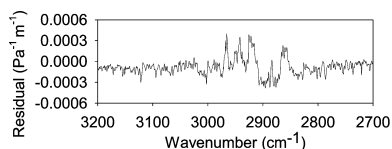


Fig. 12. Residual ($\kappa_{\text{Fit}} - \kappa_{\text{Experiment}}$) for C₃H₈ at 1000 K. This represents the difference between the data sets shown in Fig. 11.

apparent in the extrapolations is presumably an artifact resulting from the retention of the higher resolution inherent at lower temperatures. The discrepancies at the band wings are probably due to the inability of the extrapolations to capture the effects of “hot bands”, corresponding to vibrational transitions that are not populated at the lower temperatures used in determining the fitting parameters. The accuracy of the extrapolations is better for frequencies in the vicinity of the band center (Table 2). Despite these deficiencies, the errors in the integrated absorption coefficients measured at 800 and 1000 K are only about -20% and -12%, respectively. Based on calculations using AURORA [14] with the University of California, San Diego, chemical-kinetics model [15], the decomposition of propane is negligible at 800 K, but is about 8.8% at 1000 K. Thus, although the error at 1000 K appears to be smaller than at 800 K, this is only because the tendency of the extrapolation to underestimate the absorbance is partially offset by the fact that there is actually less propane at this temperature due to decomposition.

6. Summary and conclusions

The variations in the IR absorption coefficients for three combustion products (CO, CO₂, and H₂O) and one fuel (C₃H₈) were examined as functions of temperature from 300 to 1000 K. As expected, the intensities and shapes of the absorption bands of these molecules undergo dramatic changes over this temperature range, becoming broader and less intense (by as much as an order of magnitude) with the increasing population of higher energy rotational states. On this basis, it is concluded that this temperature dependence must be considered to accurately model the transfer of IR radiation and to measure the concentrations of hot gases in fires and incinerators by transmission spectroscopy. With this in mind, an extrapolation technique was developed to extend the range of molecular absorption coefficients to temperatures beyond the range for which measurements are routinely available. Experimental measurements of propane indicate that errors in the extrapolation are less than 20% based on a comparison between the integrated absorption coefficient for the extrapolated and measured data over the temperature range of interest. Thus, by employing this extrapolation procedure, the accuracy of the high temperature absorption coefficients for small gas phase molecules can be improved by as much as an order of magnitude over what would otherwise be obtained using values measured at lower temperatures. This improvement in the ability to make quantitative estimates of the absorption of radiation by fuels and other gas phase molecules at high temperatures will facilitate the validation of models directed at predicting the absorption and emission of radiation by soot in fires.

Acknowledgments

This work was partially supported by the National Research Council Postdoctoral Associate Program, the NASA Microgravity Program (Contract #C32066T; Dr. Sandra Olson, scientific officer), and the Fire Research Grants Program (Contract # 60NANB1D0075). The authors acknowledge helpful discussions with Professors

Jungho Kim and Greg Jackson of the Department of Mechanical Engineering of the University of Maryland.

References

- [1] M.F. Modest, S.P. Bharadwaj, *JQSRT* 73 (2002) 329–338.
- [2] J. DeRis, *Proc. Combust. Inst.* 17 (1979) 1003–1015.
- [3] S.P. Fuss, M.J. Hall, O.A. Ezekoye, *Appl. Opt.* 38 (1999) 2895–2904.
- [4] M.A. Brosmer, C.L. Tien, *JQSRT* 33 (1985) 521–532.
- [5] M.A. Brosmer, C.L. Tien, *ASME J. Heat Transfer* 107 (1985) 943–948.
- [6] M.A. Brosmer, C.L. Tien, *Combust. Sci. Technol.* 48 (1986) 163–175.
- [7] S.H. Park, A.J. Stretton, C.L. Tien, *Combust. Sci. Technol.* 62 (1988) 257–271.
- [8] L.A. Gross, P.R. Griffiths, J.N.-P. Sun, in: J. Wormhoudt (Ed.), *Infrared Measurements for Gaseous Measurements*, Marcel Dekker, New York, 1985, pp. 81–132.
- [9] L.S. Rothman, C. Camy-Peyret, J.-M. Flaud, R. Gamache, A. Goldman, D. Goorvitch, R. Hawkins, J. Schroeder, J. Selby, R. Wattson, *JQSRT*, in press.
- [10] L.S. Rothman, C.P. Rinsland, A. Goldman, S.T. Massie, D.P. Edwards, J.M. Flaud, A. Perrin, C. Camy-Peyret, V. Dana, J.Y. Mandin, J. Schroeder, A. McCann, R.R. Gamache, R.B. Wattson, K. Yoshino, K.V. Chance, K.W. Jucks, L.R. Brown, V. Nemtchinov, P. Varanasi, *JQSRT* 60 (1998) 665–710.
- [11] T. Fleckl, H. Jager, I. Obernberger, *J. Phys. D* 35 (2002) 3138–3144.
- [12] C.P. Tripp, R.A. McFarlane, *Appl. Spectrosc.* 48 (1994) 1138–1142.
- [13] P.M. Chu, F.M. Guenther, G.C. Rhoderick, W.J. Lafferty, *J. Res. Natl. Inst. Standards Technol.* 104 (1999) 59–81.
- [14] R.J. Kee, F.M. Rupley, J.A. Miller, M.E. Coltrin, J.F. Graciar, E. Meeks, H.K. Moffat, A.E. Lutz, G. Dixon-Lewis, M.D. Smooke, J. Warnatz, G.H. Evans, R.S. Larson, R.E. Mitchell, L.R. Petzold, W.C. Reynolds, M.W. Caracotsios, E. Stewart, P. Glarborg, C. Wang, O. Adigun, W.G. Houf, C.P. Chou, S.F. Miller, *AURORA Application User Manual—CHEMKIN Collection*, Reaction Design, San Diego, CA, 2003.
- [15] *Chemical-Kinetic Mechanisms for Combustion Applications*. University of California, San Diego, Center for Energy Research, 2002.

Comments

Joachim W. Walewski, *University of Wisconsin-Madison, USA.* (1) Am I accurate in that you need a three fit parameters (S_0 , ν_r , and p) for each absorption line, or are they unique for, e.g., a vibrational band?

(2) How many parameters does your model typically contain when compared to HITEMP?

Reply. Our model needs three fitting parameters and two variables for line-by-line, compared to 14

parameters for HITEMP [1, 2]. The detail of each parameter in HITEMP is in the Appendix A of Ref. [1].

References

- [1] L.S. Rothman, C.P. Rinsland, A. Goldman, S.T. Massie, D.P. Edwards, J.M. Flaud, A. Perrin, C. Camy-Peyret, V. Dana, J.Y. Mandin, J. Schroeder, A. McCann, R.R. Gamache, R.B. Wattson, K. Yoshino, K.V. Chance, K.W. Jucks, L.R. Brown, V. Nemtchinov, P. Varanasi, The HITRAN Molecular Spectroscopic Database and HAWKS (HITRAN Atmospheric Workstation): 1996 Edition, *JQSRT*, 60 (1998) 665–710.
- [2] L.S. Rothman, C. Camy-Peyret, J.-M. Flaud, R. Gamache, A. Goldman, D. Goorvitch, R. Hawkins, J. Schroeder, J. Selby, R. Wattson, HITEMP, The High-Temperature Molecular Spectroscopic Database, *JQSRT*, in press.



Peter Ashman, University of Adelaide, Australia.
What effect, if any, do the N₂-cooled windows

have on the gas temperature in the high-temperature cell close to the ZnSe windows? How sensitive are the fitted high-temperature spectra to any such cooling?"

Reply. To overcome cooling effects at the windows, we used a three-zone furnace, and adjusted the set point of each zone to provide nearly equal inlet and outlet gas temperatures (approximately ± 5 K). To quantify the effect of cooling, we also made thermocouple measurements of the gas temperature along the approximate axis of our cylindrical test cell, at uniform furnace settings. Measurement points started 1.3 cm from the inlet window, and were made approximately every 4 cm, up to a point 1.3 cm from the exit window. For uniform furnace set points of 401, 600, and 803 K, the measured axial temperatures and standard deviations were $(418.8 \pm 3.9, 617.7 \pm 6.9, \text{ and } 822.4 \pm 2.3)$ K, respectively. For these uniform furnace set points, the near centerline gas temperatures at 1.3 cm from the exit window were 10–15 K less than at the center of the cell. By using non-uniform set points for the three furnace zones, we should obtain more uniform gas temperatures.